CONF-781C 58--2

(For presentation at INS International Symposium on Nuclear Direct Reaction Mechanisms, Fukuoka, Japan, Oct. 25-28, 1978)

MASTER

MICROSCOPIC, SEMI-REALISTIC INTERACTIONS FOR BOTH LIGHT- AND HEAVY-ION SCATTERING

G. R. Satchler*

Oak Ridge National Laboratory**
Oak Ridge, TN 37830 U.S.A.

NOTICE
This report was prepared as an account of work sponsored by the United States Government. Neither the United States nor the United States Department of Energy, nor any of their employees, nor any of their contractors, subcontractors, or their employees, makes any warranty, express or implied, or assumes any legal liability or responsibility for the accuracy, completeness or usefulness of any information, apparatus, product or process disclosed, or represents that its use would not infringe privately owned rights.

Abstract

A review is given of the use of nucleon-nucleon effective interactions, or G-matrices, derived from realistic nucleon-nucleon forces and applied to the scattering of both light and heavy ions. Particular attention is paid to the usefulness of simple representations of these interactions. It is shown that they are remarkably successful in describing the data for both elastic and inelastic scattering.

1. Introduction

Relating nucleon-nucleus and nucleus-nucleus scattering to the underlying nucleon-nucleon (NN) interaction is an important problem. Much of the present analysis of such scattering and reactions is in phenomenological terms, using models like the optical model, collective model, etc. Such models are very useful for correlating information about nuclei from different sources and, indeed, when they are successful (as, e.g., the collective model) they give us some insight into the nature of nuclear dynamics. Nonetheless, it is of considerable interest to understand these models in terms of the individual nucleon motions and interactions. (This is what is meant by the word 'microscopic' in the title.)

Because of the strong, short-range repulsion in the NN interaction, an important first step in this program is a transformation to an effective interaction[1]. This procedure is closely parallel to what is required for a justification of the nuclear shell model[2]. One way to do this involves a two-step reduction of the full Hilbert space to the (very much smaller) model space in which we do actual calculations. The first step is to take care of the short-range repulsion (e.g. 'hard core'). This involves highly excited intermediate states, and we may reasonably hope that these are not sensitive to the particular nucleus we are studying; they are, perhaps, more characteristic of 'nuclear matter'. This leads one to some G-matrix as an effective

By acceptance of this article, the publisher or recipient acknowledges the U.S. Government's right to retain a non-exclusive, royalty-free license in and to any copyright covering the article.

DISTRIBUTION OF THIS DOCUMENT IS UNLIMITED

NN interaction to be used in the remainder of the space. This remaining space may still be too large to handle explicitly so that it has to be truncated further[3] to make calculations convenient or possible. For example, if this second truncation is to the elastic channel alone, we have the optical model. Truncation to a few strongly coupled states leads to a coupled-channels problem, perhaps with the use of the collective model for the nuclear dynamics. If the second truncation is made instead in terms of the shell model space used, its consequences can be expressed as a further modification of the effective NN interaction with the addition of what have become called 'core polarization' effects. Obviously there are variations possible in this program, but at least this is the kind of philosophy that is used. I am not sure that formal reductions of this type have really been carried through all the way to where we do actual scattering calculations without some drastic simplification at some point. One of these is the popular use in finite nuclei (in a local-density approximation) of a G-matrix characteristic of nuclear matter[4,5]; of course, the construction of a finite-nucleus G-matrix is beset with many difficulties and has to be redone, in principle, for every nucleus and for every energy studied[6].

Perhaps the most sophisticated works in this direction are due to Jeukenne, Lejeune and Mahaux[4] and Brieva and Rook[5], who concentrate on 'average' properties of the interaction. (See also Lerner and Redish[6] who studied one nucleus in some detail.) Figure 1 shows some results[5] based upon Hamada and Johnston's potential; the agreement with experiment is very good for an <u>ab initio</u> calculation. (It also emphasises another feature we shall return to, that theoretical potentials do not necessarily have the conventional Woods-Saxon shape!)

One aspect of this program, with which I am particularly concerned here, is to look for an approximate effective NN interaction which is sufficiently simple that it may be easily and widely used. (Hence the modifier 'semi-' in the title!) If successful, this would give us a unified description of NN, N-nucleus and nucleus-nucleus scattering, a model which had predictive power and which could be used to probe nuclear structure. There is certainly no guarantee that it is possible to achieve this simple objective, however it is well worth trying. I report here the results of some attempts in this direction which are very encouraging.

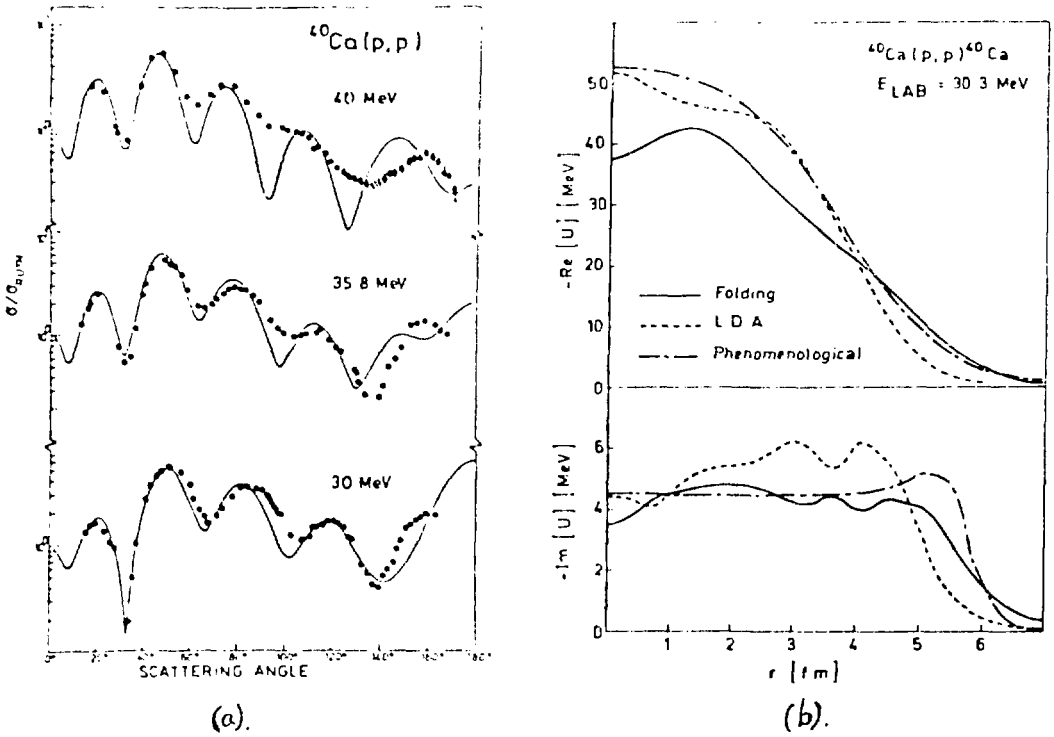

Fig. 1. (a) Proton scattering calculated[5] with a G-matrix from the Hamada-Johnston potential. (b) Real and imaginary parts of the potential ('LDA' corresponds to taking zero-range for G, 'Folding' includes the finite-range of G, 'Phenomenological' is a Woods-Saxon potential.)

2. Properties of the Effective Interaction

A formally-derived effective NN interaction or G-matrix has many undesirable features as something to be used in extensive model calculations; it is non-local and energy-dependent, it does not have an analytic form, and it depends upon the positions and momenta of the two interacting nucleons within the nucleus. The hope is that some suitable average of this object can be represented by some relatively simple, local, function. In this way, the object we seek is 'effective' at two levels:

$$v_{NN,bare} \rightarrow G; \; \bar{G} \rightarrow v_{NN,eff}. \tag{1}$$

(In what follows I shall frequently refer simply to 'G' even when I usually mean the averaged $\bar{G}$.) We are encouraged to believe that this can be done by the relative success for both elastic and inelastic proton scattering of the

earlier use[7,8] of the Moszkowski-Scott separation method which says[9] that a first approximation to G is the long-range part of $v_{NN,bare}$. This gives us a $v_{NN,eff}$ which is both local and simple if we use one of the popular NN potentials such as Reid's or Hamada-Johnston's.

The dependence of G upon the positions of the two interacting nucleons within the nucleus is expressed in most treatments by a form of local density approximation (LDA) which makes the effective interaction density-dependent. In its simplest form[4,5] this takes $G(\underset{\sim}{r}_1,\underset{\sim}{r}_2)$ to be the same as the $G^{(\infty)}(\underset{\sim}{r}_{12};\rho)$ for infinite nuclear matter at the same density $\rho(\bar{\underset{\sim}{r}})$ as is found at the centre of gravity $\bar{\underset{\sim}{r}} = \frac{1}{2}(\underset{\sim}{r}_1 + \underset{\sim}{r}_2)$ of the two interacting nucleons within the finite nucleus, $\rho = \rho(\bar{\underset{\sim}{r}})$. This ignores the effects of density gradients on G. This may not be so good in the nuclear surface since the 'range' of G is not much smaller than the surface thickness of nuclear density distributions. The resulting density-dependence is not small; Fig. 2 shows examples from the work of Jeukenne, Lejeune and Mahaux[4].

Figure 2 also illustrates the energy dependence, there expressed as a dependence on the bombarding energy of the nucleon incident on nuclear matter after averaging over the (Fermi) momentum distribution of the target nucleons.

The effective interaction for scattering differs from that for two bound nucleons in that it has an imaginary part; when one nucleon is above the Fermi surface, there are always 2-particle, 1-hole states degenerate with the initial state into which the nucleons can scatter. Of course, this imaginary part is essential for the optical model for elastic scattering; it also is important for determining the angular distributions for inelastic scattering. Calculating G for nuclear matter in the appropriate way[4,5] automatically generates this imaginary part. However, it is perhaps more questionable to use the LDA in applying this to finite nuclei than it is for the real part. The spectrum of excited states for a finite nucleus shows strong shell effects and collective effects (due to the possibility of shape oscillations) which are not present for the Fermi gas of nuclear matter. It remains to be seen how important these are, but it may be significant that current calculations[4,5] are less successful in reproducing the imaginary part of the nucleon optical potential than the real part. However, explicit calculations of the absorptive processes for a finite nucleus (see Ref. 10 for example) are lengthy and only moderately successful; perhaps we will have to be content with a semiphenomenological approach to the imaginary

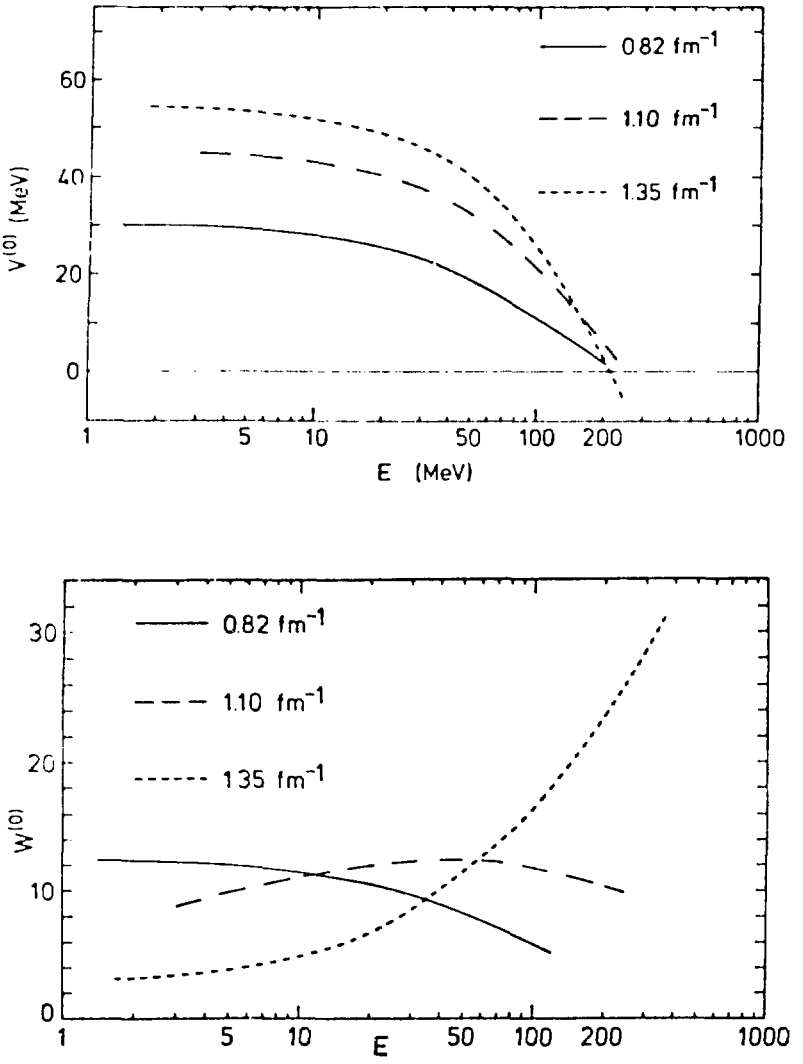

Fig. 2. Density and energy dependence of real ($V^{(o)}$) and imaginary ($W^{(o)}$) parts of G-matrix for nuclear matter based[4] upon Reid's potential. Plotted is the volume integral of $\bar{G}$ times the nuclear density. Fermi momenta of 0.82, 1.10 and 1.35 fm^{-1} correspond to densities of 0.22, 0.54 and 1 times 'normal' density.

interaction, based upon theory but normalized by comparison with data (see also Ref. 11 for example).

The effective interaction is, of course, spin- and isospin-dependent.

The central parts may be written[1,7)]

$$v^c_{eff} = v_{00}(\underset{\sim}{r}_1,\underset{\sim}{r}_2) + v_{10}(\underset{\sim}{r}_1,\underset{\sim}{r}_2)\sigma_1\cdot\sigma_2 + v_{01}(\underset{\sim}{r}_1,\underset{\sim}{r}_2)\tau_1\cdot\tau_2 + v_{11}(\underset{\sim}{r}_1,\underset{\sim}{r}_2)\sigma_1\cdot\sigma_2\tau_1\cdot\tau_2, \tag{2}$$

and, in addition, there are spin-orbit and tensor components[1,12)]. Elastic scattering is dominated by v_{00}, while the asymmetry component (~ (N-Z)/A) of nucleon-nucleus potentials and the charge-exchange interaction for (p,n) reactions arises primarily from v_{01}. The other v_{ST} terms and the tensor terms are most easily seen in inelastic scattering transitions which select the appropriate $\Delta S, \Delta T$. The two-body spin-orbit interaction manifests itself in the one-body spin-orbit coupling of the nucleon-nucleus optical potential[13)] as well as often playing an important role in some inelastic transitions[12)].

3. Folding Calculations for Nucleons

In order to construct a one-body optical potential (elastic scattering) or transition potential (inelastic scattering) for nucleon scattering, something like the procedure now to be described must be followed. The potential felt by the scattered nucleon at position $\underset{\sim}{r}_1$ starts out being non-local, as well as dependent upon the bombarding energy. To lowest order, it is given by

$$U(\underset{\sim}{r}_1,\underset{\sim}{r}_1';E) = \delta(\underset{\sim}{r}_1-\underset{\sim}{r}_1') \int \rho(\underset{\sim}{r}_2)G_D(\underset{\sim}{r}_1,\underset{\sim}{r}_2;E)d\underset{\sim}{r}_2 + \rho(\underset{\sim}{r}_1,\underset{\sim}{r}_1')G_{EX}(\underset{\sim}{r}_1,\underset{\sim}{r}_1';E) \tag{3}$$

where $\rho(\underset{\sim}{r})$ is the one-body density (or transition density) of the target nucleus and $\rho(\underset{\sim}{r},\underset{\sim}{r}')$ is the corresponding density matrix, so that $\rho(\underset{\sim}{r}) \equiv \rho(\underset{\sim}{r},\underset{\sim}{r})$. Further, G_D is that combination of even and odd interactions[7)] appropriate for the direct transition (e.g. the S=T=0 combination in the sense of Eq. (2) for elastic scattering from an even target with N = Z) and G_{EX} is the combination for exchange scattering (i.e. the same except for changing the sign of the odd components).

It is convenient to define an equivalent local potential U_{LE}, for example by using the relation (where $\phi(\underset{\sim}{r})$ is the scattering wave function)

$$U_{LE}(\underset{\sim}{r}_1)\phi(\underset{\sim}{r}_1) = \int U(\underset{\sim}{r}_1,\underset{\sim}{r}_1')\phi(\underset{\sim}{r}_1')d\underset{\sim}{r}_1' \tag{4}$$

and then making a local energy approximation for $\phi(\underset{\sim}{r}_1')$ in the exchange term. This gives

$$U_{LE}(\underset{\sim}{r}_1;E) \approx \int \rho(\underset{\sim}{r}_2)G_D(\underset{\sim}{r}_1,\underset{\sim}{r}_2;E)d\underset{\sim}{r}_2 + \int \rho(\underset{\sim}{r}_1,\underset{\sim}{r}_1')G_{EX}(\underset{\sim}{r}_1,\underset{\sim}{r}_1';E)j_0(k|\underset{\sim}{r}_1-\underset{\sim}{r}_1'|)d\underset{\sim}{r}_1', \tag{5}$$

where k is the wavenumber for the local kinetic energy of the nucleon at position $\underset{\sim}{r}_1$. This may be further simplified by introducing the Slater approximation to the density matrix

$$\rho(\underset{\sim}{r},\underset{\sim}{r}') \approx \rho(\bar{\underset{\sim}{r}}) \frac{3}{sk_F} j_1(k_F s) \tag{6}$$

where $\bar{\underset{\sim}{r}} = \frac{1}{2}(\underset{\sim}{r}+\underset{\sim}{r}')$, $s = |\underset{\sim}{r}_1-\underset{\sim}{r}_1'|$ and k_F is the Fermi momentum corresponding to the density $\rho(\bar{\underset{\sim}{r}})$. If we now substitute the nuclear matter $G^{(\infty)}(\underset{\sim}{r}_{12};\rho(\bar{\underset{\sim}{r}});E)$ for matter of density $\rho(\bar{\underset{\sim}{r}})$, in place of the finite nucleus $G(\underset{\sim}{r}_1,\underset{\sim}{r}_2;E)$, the integrals in (5) become

$$\begin{aligned} U_{LE}(\underset{\sim}{r}_1;E) &\approx \int \rho(\underset{\sim}{r}_1+\underset{\sim}{s})G_D^{(\infty)}(s;\rho;E)d\underset{\sim}{s} \\ &+ \int \rho(\underset{\sim}{r}_1 + \tfrac{1}{2}\underset{\sim}{s})G_{EX}^{(\infty)}(s;\rho;E) \frac{3}{sk_F} j_1(k_F s)j_0(ks)d\underset{\sim}{s} \end{aligned} \tag{7}$$

and can easily be done numerically using previously calculated tables of values for the $G^{(\infty)}$. (See also Love[25] for a zero-range version of this exchange term, obtainable here by assuming the product $(G_{EX}j_1j_0)$ has a sufficiently short range that we may approximate $\rho(\underset{\sim}{r}_1 + \frac{1}{2}\underset{\sim}{s}) \approx \rho(\underset{\sim}{r}_1)$ and remove it from the integral.)

Brieva and Rook[5] followed this prescription (7) to obtain elastic results such as those shown in Fig. 1. This has recently been extended[14] to inelastic scattering from a rotational nucleus by using a deformed density distribution. Figure 3 shows results for ^{154}Sm(p,p'); the only parameters which enter are those for the density distribution and these were constrained to values taken from electron scattering measurements plus the assumption that $\rho_n = (N/Z)\rho_p$. The fit to the data is astonishingly good for a calculation free of adjustable parameters. (The dashed curves show the effects of changing the deformation parameters.)

The results of Jeukenne, Lejeune and Mahaux[4], although derived somewhat differently, could be viewed as obtained in the same way with the additional assumption that G is of sufficiently short range that the densities ρ vary little over its range. Then the nucleon potential (7) has the form

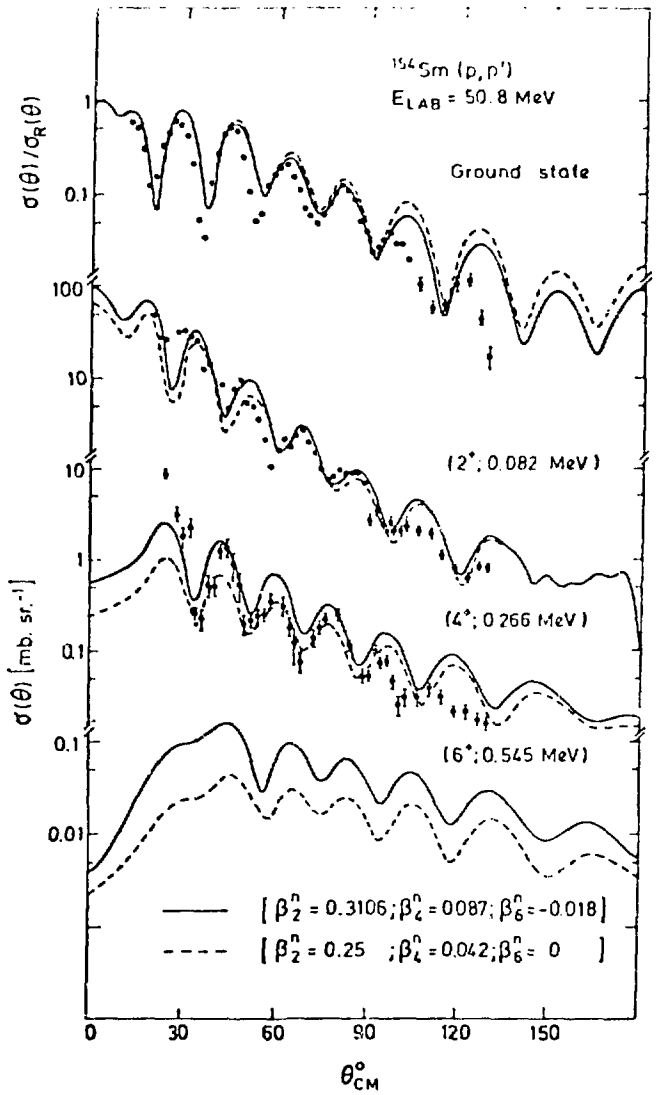

Fig. 3. An essentially parameter-free calculation of inelastic proton scattering[14].

$$U(\underset{\sim}{r}_1,E) = \rho(\underset{\sim}{r}_1)J(\rho(\underset{\sim}{r}_1);E) \tag{8}$$

where J is the 'volume integral' of $G^{(\infty)}$ (in which direct and exchange parts are not separated),

$$J(\rho,E) = \int G^{(\infty)}(\underset{\sim}{r}_{12};\rho;E)d\underset{\sim}{r}_{12}. \tag{9}$$

(It is these $U = V^{(o)} + iW^{(o)}$ which are plotted in Fig. 2 for various densities.) The approximation (8) is poor in the nuclear surface, as they realised[4], and results in the potentials U(r) having too small mean square radii. This deficiency is corrected by the full folding expression (7).

4. Simplified Effective Interactions

Here we are concerned with simple representations of the effective interaction, the second stage symbolized in Eq. (1). By this we mean representing the $G^{(\infty)}(s;\rho;E)$ in terms of simple functions such as Yukawas and Gaussians. In this way, we can avoid the need for a completely numerical representation for G, making calculations easier and faster.

The earliest attempts assumed that G could be replaced by simple potentials that fitted low-energy NN scattering (and the deuteron properties). However, it was demonstrated[8] that these were somewhat too strong and gave too deep optical potentials (both for nucleons and for heavy ions[15]) and too large inelastic cross sections. A later attempt[7,8] approximated G by the long-range part of the S-state component of a realistic NN potential such as the Hamada-Johnston. This was quite successful for nucleon scattering but overestimated heavy-ion potentials[15] by more than a factor of 2. (It is now realised that the latter was due to the complete neglect of odd-state forces, which resulted in the interaction having a spurious long-range component from the OPEP.)

A more sophisticated approach[16] led to an effective interaction that we shall call M3Y; in it a sum of 3 Yukawa terms were found (for each component of the force) which would reproduce realistic oscillator G-matrix elements. One term was fixed to be the OPEP. The next shorter range was chosen to be 0.4 fm to represent multi-pion exchange and the third term was arbitrarily chosen with a range of 0.25 fm. Thus two strength coefficients were left to be adjusted for each component. For the particular interaction we discuss here, the singlet- and triplet-even matrix elements were obtained from the Reid potential, while for the odd-states, the Elliott or 'Sussex' matrix elements were used. As an example, for the S=T=0 term in Eq. (2) this results in the expression

$$v_{00}(s) = \left[7999\,\frac{e^{-4s}}{4s} - 2134\,\frac{e^{-2.5s}}{2.5s}\right] \text{MeV}. \qquad (10)$$

(Note the absence of an OPEP contribution from this expression!)

This represents the interaction G_D for the direct term of Eq. (3). Note that since the G-matrix was in an oscillator representation, we do not have an explicit dependence on either density or energy. Indeed, this M3Y interaction corresponds to a certain average over a range of densities and kinetic energies determined by the oscillator basis used. In addition, from its construction, it is real and the imaginary interaction must be introduced phenomenologically.

There is a corresponding expression for G_{EX}, in which the odd-state contributions have opposite sign. This may be used as it stands if the exchange terms of Eq. (3) are calculated explicitly[1,7,16]. However, the calculations are greatly simplified if the exchange terms are treated approximately, for example in the way that led to Eq. (7). An alternate and simpler treatment[17] leads to the use of a zero-range pseudopotential to represent exchange so that v_{eff} is replaced by

$$v'_{eff}(s;E) = v_{eff}(s) + \hat{J}(E)\delta(\underset{\sim}{s}). \tag{11}$$

The strength $\hat{J}(E)$, which may be obtained by normalizing against 'exact' calculations of the exchange terms[18], depends sensitively on the spin-, isospin-character (i.e. S,T in Eq. (2)) but only varies weakly with the energy E. For example, for E = 10 MeV, the pseudopotential for S=T=0 to be added to Eq. (10) has $\hat{J}_{00} = -262$ MeV fm^3 and this only varies by a few percent over the range E ~ 5 to 20 MeV. The effective interaction $v'_{eff}(s)$ of Eq. (11) can then be folded with the nuclear density or transition density to give the potential,

$$U_{LE}(r;E) = \int \rho(\underset{\sim}{r}+\underset{\sim}{s})v'_{eff}(s,E)d\underset{\sim}{s}. \tag{12}$$

A nuclear-matter G-matrix interaction has been represented in a similar way. This G was obtained by Eisen and Day[19] from the Reid potential and applied successfully to alpha elastic scattering in the LDA of Eq. (7). It is local (and real) but explicitly and strongly density-dependent. Its oscillator matrix elements were fitted by a similar sum of 3 Yukawa terms by Love the density-dependence can be expressed in the form

$$v_{eff}(s,\rho) = v_1(s) + v_2(s)\ e^{-\alpha\rho}, \tag{13}$$

which has some calculational convenience. This interaction has been found to give results very similar to those obtained with the M3Y interaction. For example, Fig. 4 shows almost identical results for the folded potential for $^{16}O + ^{60}Ni$ near the strong absorption radius. (This figure also indicates that the density dependence is important by comparing results in which either the density of ^{16}O or that of ^{60}Ni were neglected.)

The nuclear matter G-matrix of Brieva and Rook[5] has also been given a simple spatial representation recently[20], as sums of 5 Gaussian terms fitted to the G for several densities.

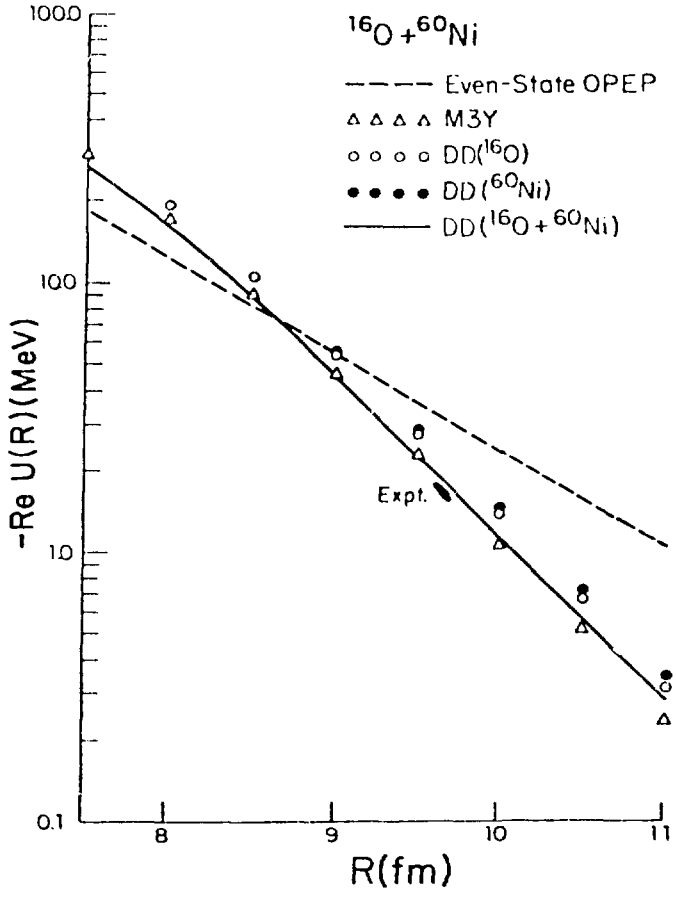

Fig. 4. Folded potentials for $^{16}O + ^{60}Ni$ near the strong absorption radius (R ≈ 9.6 fm). M3Y = interaction (10), (11); DD = one of the form (11), (13) based on Day's G-matrix[19]. The legend indicates which densities were included for the latter[39].

5. Applications to Nucleon Scattering

The M3Y interaction has not been applied in any detail to nucleon elastic scattering, but Fig. 5 shows examples for ^{60}Ni based upon the form (11) and (12). Only the real, central potential is predicted; the imaginary and spin-orbit terms were simply taken from the global potential of Becchetti

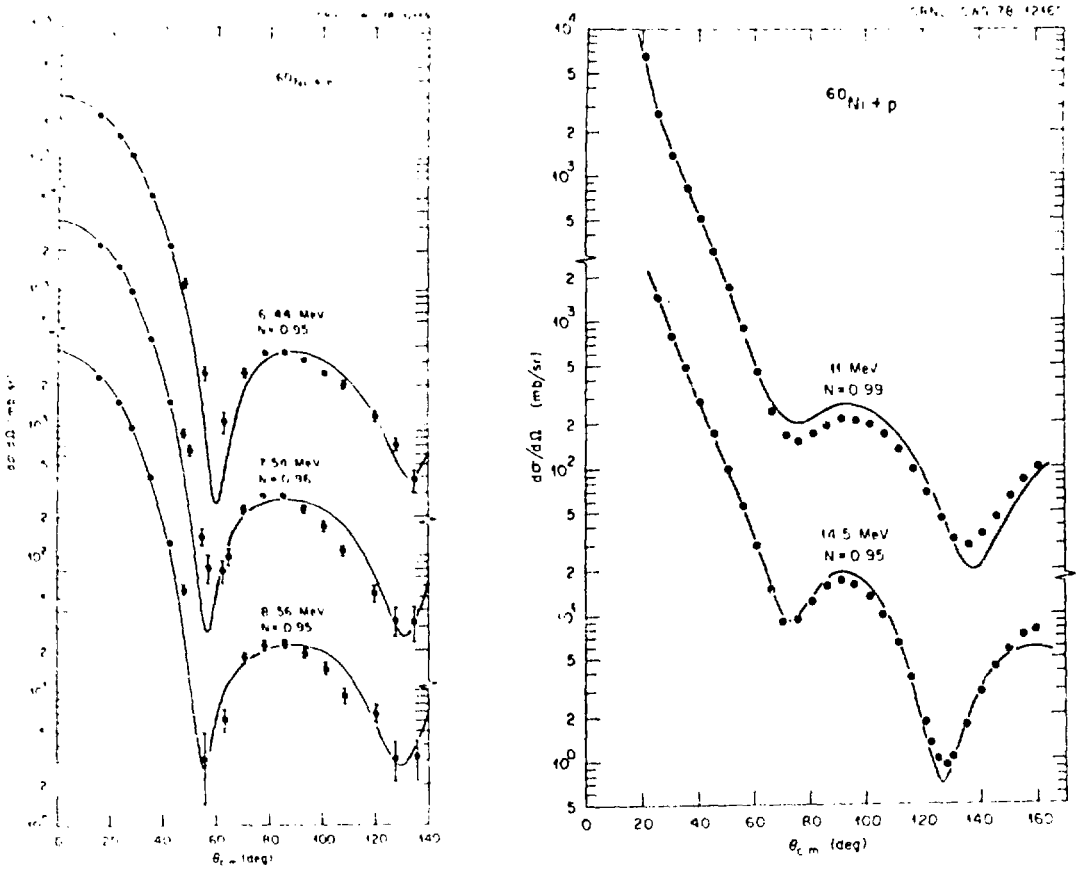

Fig. 5. Comparison with data of elastic cross sections for folded real potential from M3Y interaction (plus imaginary and spin-orbit terms from Becchetti-Greenlees global model).

and Greenlees. The agreement with experiment is satisfactory, but not as good as can be obtained with a phenomenological Woods-Saxon potential. The theoretical real potential appears to have a mean square radius which is slightly too small. This may be due to a deficiency of the zero-range pseudopotential (11) used for the exchange. A treatment of exchange like that of Eq. (7) does result in a slightly larger radius. The deficiency does not appear to be due to a mistreatment of the density-dependence because the interaction based upon Day's G-matrix[19] gives almost identical results.

Applications to an (n,n') excitation and a (p,n) isobar transition are shown in Fig. 6. The (n,n') case, predominantly S=T=0, shows another

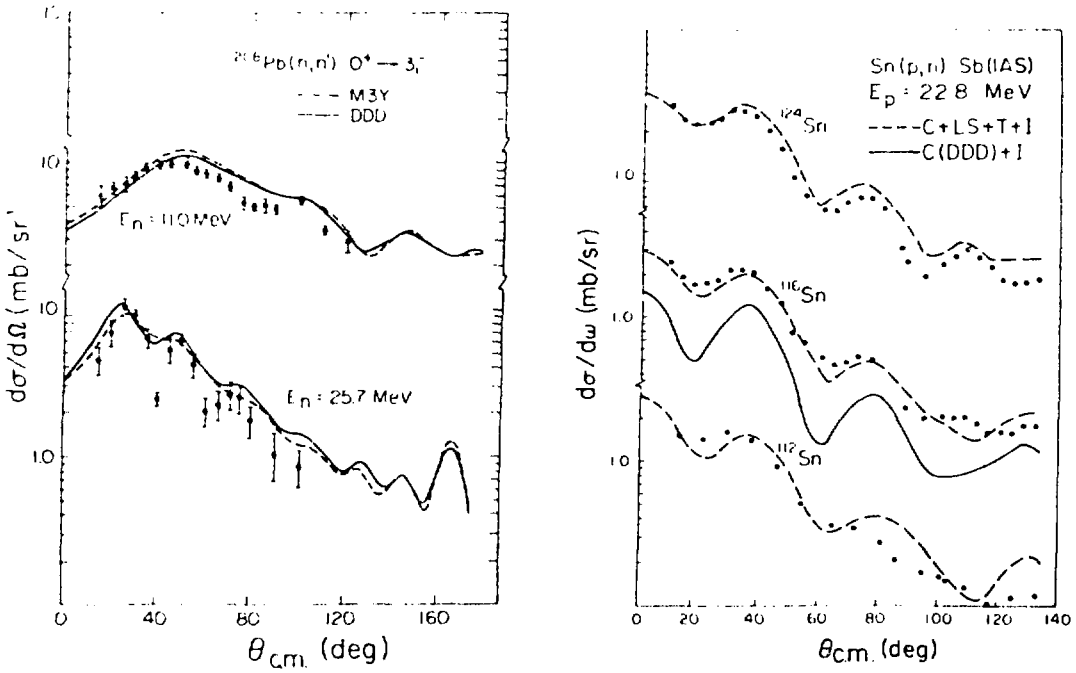

Fig. 6. Microscopic predictions[21,22] for (n,n') and (p,n) cross sections compared to data. Dashed curves: the M3Y interaction; solid curves (DDD): based on Day's density-dependent G-matrix[19]. Exchange was calculated 'exactly'.

example of the similarity between cross sections predicted by M3Y and the interaction based upon Day's G-matrix. However, the (p,n) transition (S=0,T=1) indicates that this isovector component of the latter interaction is too weak. The (n,n') was calculated[21] using RPA transition densities known to be in agreement with electron scattering and B(EL) values. The (p,n) isobar transition used[22] a neutron excess generated from the shell model.

When we consider inelastic transitions for non-closed shell nuclei and we use truncated shell model wavefunctions, the amplitudes usually have to be supplemented by so-called 'core polarization' contributions. These are the same contributions that necessitate the use of effective charges in shell model calculations. They may be calculated simply and phenomenologically[23] or microscopically but with more effort[24]. This is illustrated for a simple case in Fig. 7. With a simple $(d_{5/2})^2$ configuration, the M3Y interaction predicts a cross section too small by a factor of 4. Adding the

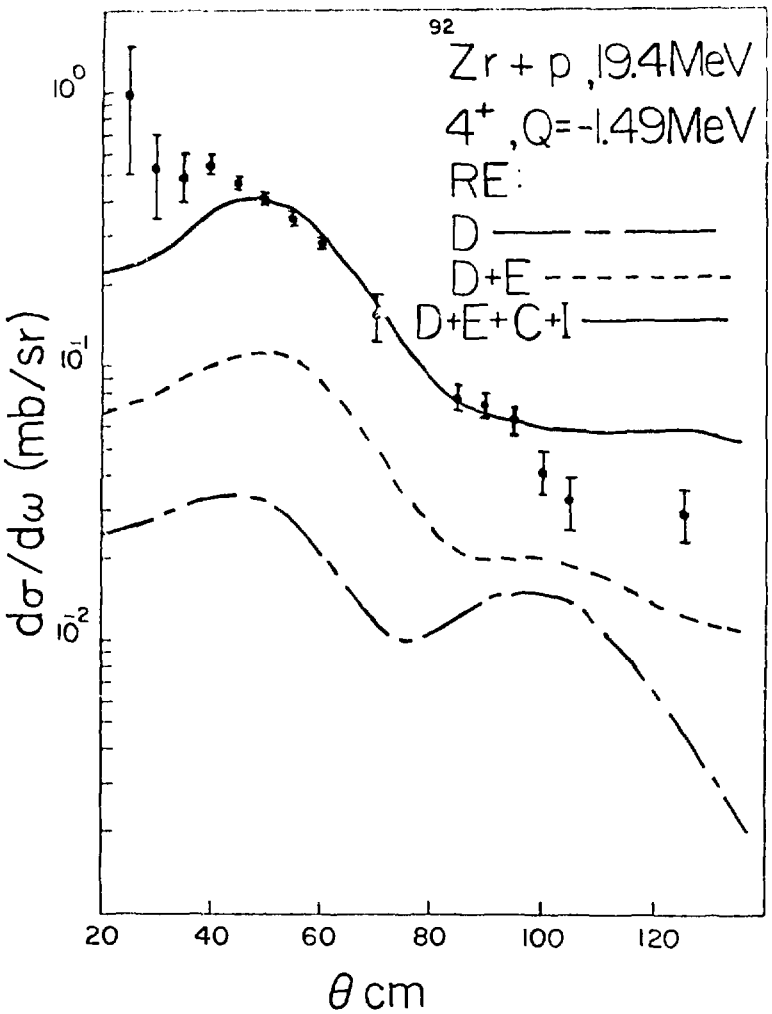

Fig. 7. Cross sections calculated with the M3Y interaction (D+E) assuming $(d_{5/2})^2$ neutrons, and with core polarization (C). (D = direct, E = exchange).

phenomenological core polarization amplitude brings agreement with the data. In this case, the phenomenological 'core' part is comparable to the part being calculated microscopically; the interference between them is very important. (Figure 7 also illustrated the importance of the exchange (E) term for the higher multipoles[7]. Adding it to the direct term (D+E) gives much more cross section than the direct (D) term alone.)

6. Folding for Composite Projectiles

When the projectile is composite (e.g. a 'heavy ion'), the folding formulae (7) or (12) must be extended to include integrating over the projectile density distribution (the so-called 'double folding'). For example, Eq. (12) becomes

$$U_{LE}(\underset{\sim}{R};E) = \iint \rho_1(\underset{\sim}{r}_1)\rho_2(\underset{\sim}{r}_2)v'_{eff}(\underset{\sim}{r}_{12};E)d\underset{\sim}{r}_1 d\underset{\sim}{r}_2 \tag{14}$$

where the coordinates are defined in Fig. 8, and we have assumed the zero-range pseudo-potential (11) to account for the interchange of one nucleon from each nucleus. (Since in most cases it is the potential for peripheral collisions that is important, it is reasonable that this single nucleon exchange should be the dominant effect of antisymmetry between the two nuclei.) Eisen and Day in their work[19] on alpha scattering used a double-folded generalization of Eq. (7). It has been found[25] that one version of this approach predicts somewhat larger exchange contributions than the approximation (11). A similar treatment of exchange has recently been advocated[26] for alpha scattering.

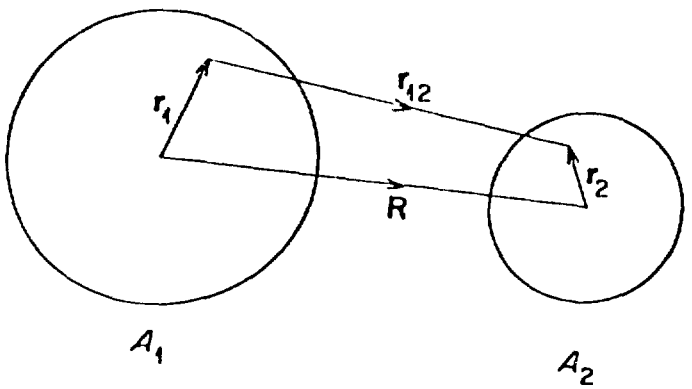

Fig. 8. Coordinates for double-folding integrals.

When an explicitly density-dependent interaction is being used, the question arises as to what density to use when two composite nuclei collide. The form (13) factorizes in a useful way if we choose the ρ that G depends upon to be simply

$$\rho = \rho_1(\underset{\sim}{r}_1) + \rho_2(\underset{\sim}{r}_2),$$

rather than, say, $\rho_1 + \rho_2$ evaluated at $\bar{\underset{\sim}{r}} = \frac{1}{2}(\underset{\sim}{r}_1 + \underset{\sim}{r}_2)$. Of course, the whole approach must be wrong if the results are very sensitive to the choice we

make. A more basic problem concerns the very definition of G in this situation; for example, we have two pieces of nuclear matter moving relative to one another. Nonetheless, we ignore these problems for the present and simply ask how good is an effective interaction such as the M3Y.

The most direct measure we have of the densities to be used in the folding model comes from electron scattering. This only tells us about the charge distribution, i.e. primarily the proton distribution. To extract the distribution of proton centers ρ_p, it is important to unfold the finite charge distribution of the proton (and the neutron). For example, the folded potential for $^{40}Ca + ^{40}Ca$ at the strong absorption radius increases by 54% if we forget to do this. Our information about neutron distributions ρ_n is less direct (although analyses of recent high energy proton scattering are promising). For nuclei with N = Z it is probably adequate to take $\rho_n = \rho_p$. For other nuclei, we resort to the shell model with the same sized potential-well for both neutrons and protons but with well-depths adjusted to yield the correct separation energies for the least-bound nucleons. For the closed-shell nuclei $^{40,48}Ca$, ^{90}Zr and ^{208}Pb we also use the Hartree-Fock densities of Negele.

Since the real potential for strong-absorption scattering is only important for nuclear separations corresponding to a very small overlap of the two densities, the range of the interaction is very important. This is illustrated by Fig. 9 which shows the volume integral required for v_{eff} to produce the correct potential for $^{40}Ca + ^{40}Ca$ as the range of v_{eff} is varied. This implies, for example, that one would have to use with great caution schematic interactions such as Skyrme's which were derived in situations where their range was of little consequence. This sensitivity to range also explains why it is important to treat correctly the long-range OPEP. The early use[7,8] of the long-range part of the even-state Hamada-Johnston potential contained a spurious term from the OPEP; because of its range (1.4 fm) this contributed a disproportionate amount to the tails of heavy-ion potentials[15]. Figure 4 shows that this spurious term alone gives a potential larger than the empirical one near the strong absorption radius.

We may ask what parts of the density distribution are sampled in a folding calculation. The main interest is in the potential at the strong absorption radius where typically the half-density points of the two nuclei are still separated by about s = 3 fm. Figure 10 shows how this potential

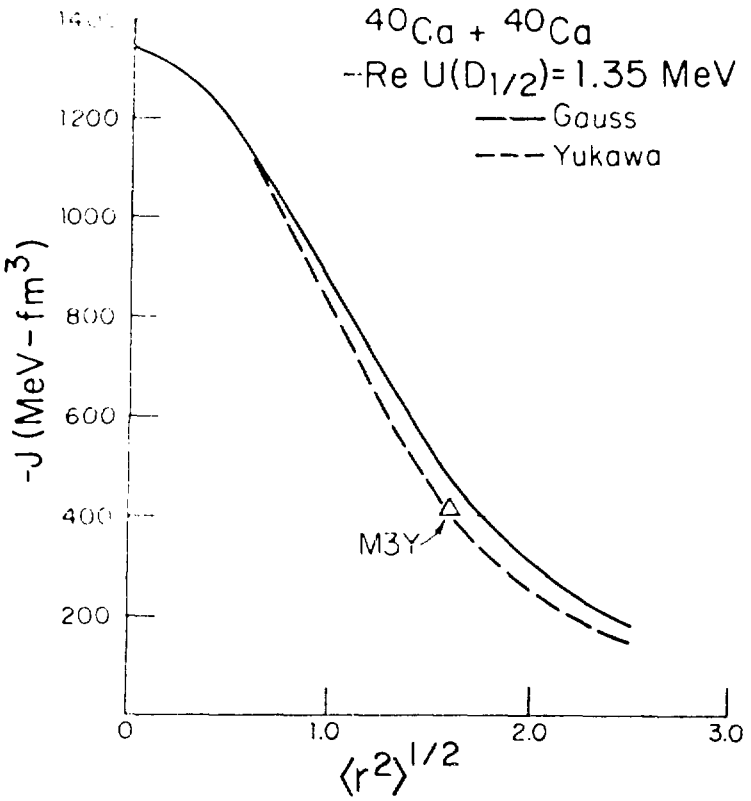

Fig. 9. Variation of volume integral of a single Gauss or Yukawa term with its mean square radius needed to give the empirical potential at the strong absorption radius ($D_{1/2} \approx 10.6$ fm).

changes if we put the two densities equal to zero at n times the diffuseness parameter a beyond the half density radius C; i.e. we put $\rho_i(r) = 0$ if $r > c_i + na_i$. The calculation is for $^{84}Kr + ^{209}Bi$ with $a_1 = a_2 = 0.5$ fm. The strong absorption radius is about R = 14.2 fm. If we are to attain the potential at this radius correct to 1%, the densities must be carried out to $r \approx c + 9.5a$ (where they are $\sim 10^{-4}$ of their central values and extend well into the other nucleus). We see that 20% of the potential comes from ρ at $r > c + 5.4a$ where the density tail of one nucleus has reached the half-density region of the other nucleus. In other words, it is not just the extreme tails of the ρ_i that are involved but their whole surface regions.

7. Applications to Alpha-Particle Scattering

First we consider alpha scattering. Although many folding calculations have been made for alphas with a variety of interactions, including that of Eisen and Day[19] (see, for example, Ref. 27), rather few applications of the M3Y interaction have been made. These include the $\alpha + \alpha$ system, for which the folded potential obtained was found to be almost exactly the same as the potential previously found[28] to reproduce accurately the $\alpha + \alpha$ phase shifts

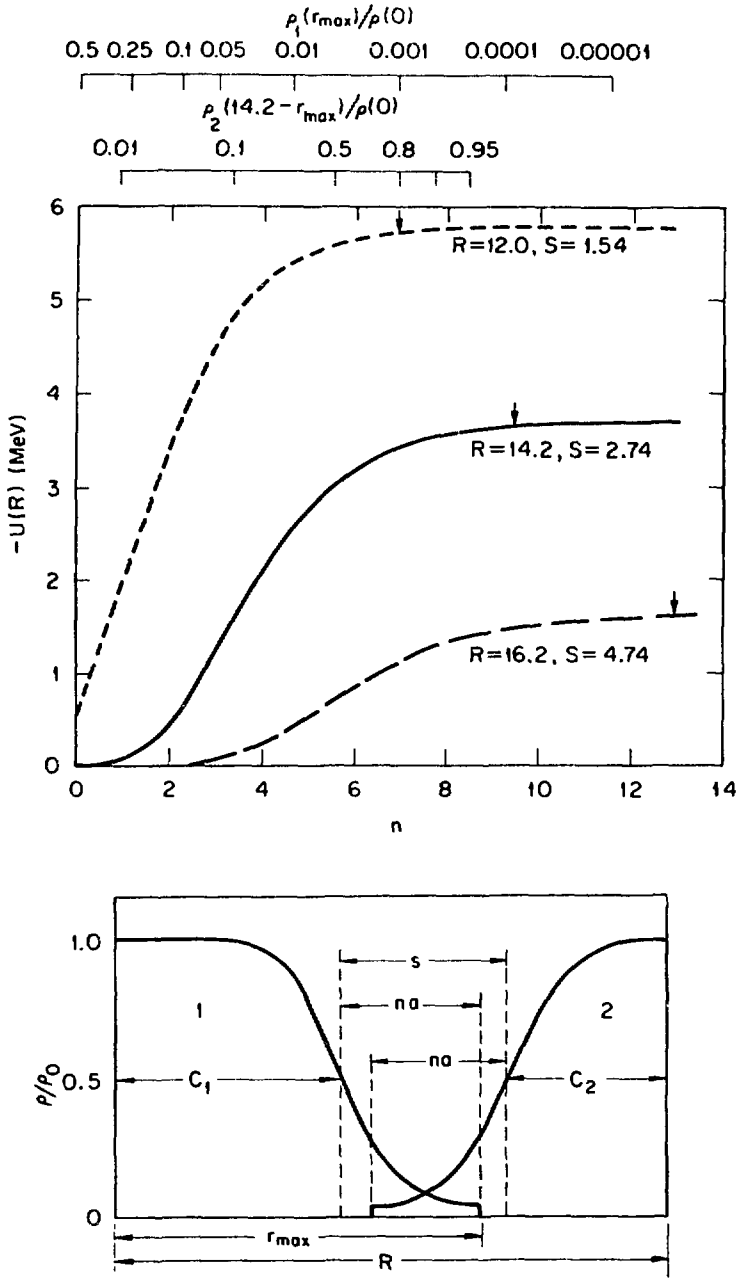

Fig. 10. Strength of folded potential for $^{84}Kr + ^{209}Bi$ separated by R fm when their densities are cut off at $r = r_{max} = c_i + n\, a_i$. Here $a_i = 0.5$ fm. (Curve for R = 16.2 is × 10, curve for R = 12 is × $\frac{1}{10}$).

up to 40 MeV.

Perhaps the most interesting case is $\alpha + {}^{40}Ca$ which, at energies around 30 MeV, exhibits the so-called anomalous large-angle scattering (ALAS) (see Fig. 11). It is now known[29] that this can be understood as a simple

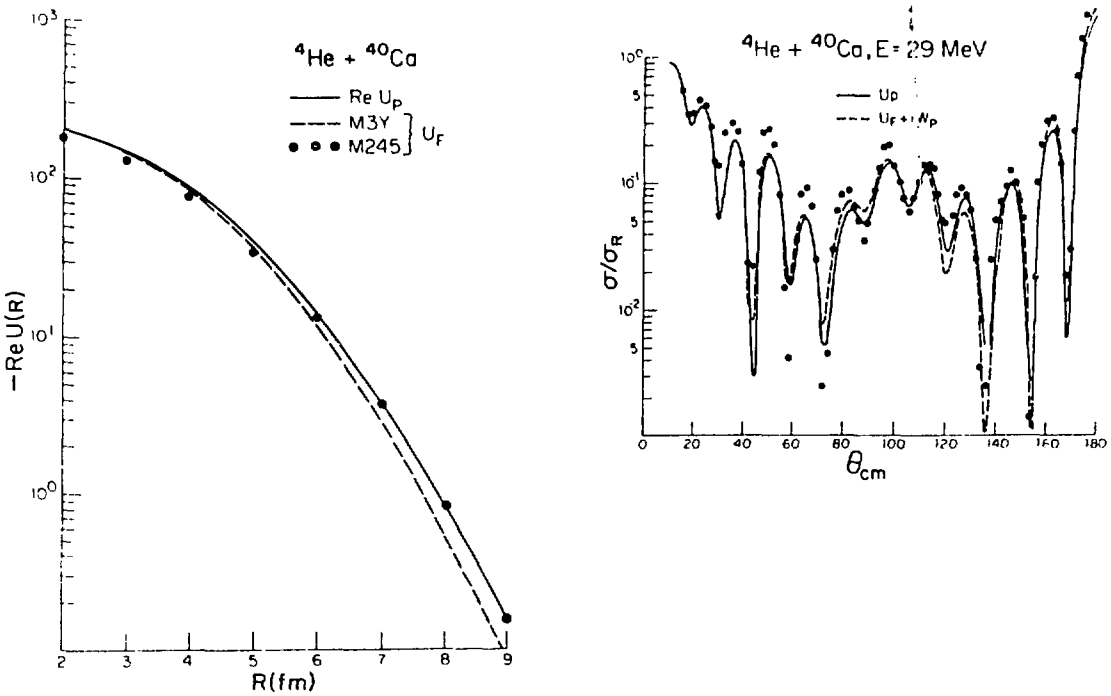

Fig. 11. Real potentials and cross sections for $\alpha + {}^{40}Ca$. U_P is the phenomenological (Woods-Saxon)$^{2.65}$ potential[29]; U_F is the folded potential[31]. (M245 is an interaction like M3Y but with a slightly longer range[31].)

potential scattering phenomenon arising from relatively weak absorption in the nuclear interior. This allows for a wave to be reflected from the inner, centrifugal barrier without being totally absorbed which is responsible for the ALAS[30]. (Thus, the scattering is 'anomalous' only in the sense that the absorption for this system in this energy region is less than 'usual'.) What is found[31] is that a folded potential using the M3Y interaction (in the form (10) and (11)) gives very closely the same real potential (see Fig. 11) as the phenomenological one deduced[29] from the data. (Indeed, fits to the data like that shown in Fig. 11 can be obtained with just <u>one</u> adjustable parameter

by taking the imaginary potential to have the same shape as the folded real one and adjusting its strength.) There are two interesting features:

(i) The phenomenological potential[29] has a Woods-Saxon form raised to the 2.65 power, thus emphasising again that folded potentials in general have shapes different from the simple Woods-Saxon one.

(ii) The real potential required[29] to fit the data is deep (~ 290 MeV at r = 0) which agrees with the folding model. Since the scattering here is sensitive to the potential at smaller radii, this implies that the folding model with this interaction is reproducing the correct potential even in regions where the α and ^{40}Ca have complete overlap.

Two other points should be noted. First, that the density-dependent interaction derived from Day's G-matrix[19] gives a very similar folded potential. Secondly, there are indications[31] both from the elastic and the inelastic scattering that the folded potentials would give improved fits if their mean square radii were increased slightly. This may be further evidence that the zero-range approximation (11) to exchange is not fully adequate. Preliminary results suggest that an improved approximation[25,26] in the spirit of Eq. (7) gives better results.

8. Applications to Heavy-Ion Scattering

Many applications to heavy-ion scattering data have been made using the folding model with the M3Y interaction and will be discussed elsewhere[32]. Most of the applications have been for elastic scattering, although some successes have been reported for inelastic scattering also (see Refs. 37 and 38 for example). In most cases the data only determine the potential at some strong absorption radius. Figure 12 illustrates this; the shaded band encompasses many Woods-Saxon potentials which fit the data equally well[33]. We see that the potential is determined primarily at r ≈ 10.5 fm. The calculated[33] folded potential from M3Y reproduces the value here to 2%. (Figure 4 provides another example for a similar system.)

To summarize a recent review[32] of applications of M3Y, we list in Table 1 the systems studied, together with the factors N by which the real folded potential had to be multiplied in order to optimize the fit to the data. (In each case, a Woods-Saxon imaginary potential was used with a minimum adjustment of its parameters.) The value N = 1.0 means that the model is successful. Undoubtedly, some of the fluctuations of N about unity are due either

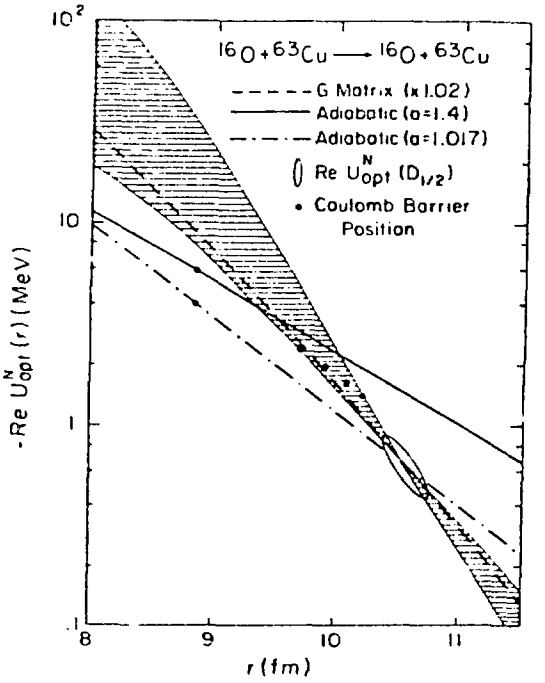

Fig. 12. Potentials near strong absorption radius ($D_{1/2} \approx 10.5$ fm) which fit the data[33]. Shaded area includes Woods-Saxon potentials. Dashed curve is the folded potential from M3Y interaction.

to uncertainties in the densities used or to idiosyncracies in the data being fitted. However, the trend is for $N \approx 1.1$ with deviations mostly around 10%, quite a remarkable success for such a simple model and interaction. (We may say, in another sense, that the interaction is indeed 'effective'!)

Figure 13 shows the fits for some light heavy-ion systems. Figure 14 provides some evidence that the scattering is sensitive to the value of the real potential. The data for this particular energy are anomalous in requiring a deeper real potential than is needed at other energies; Fig. 15 shows that the potential adjusted to fit the 74-MeV data ($N = 1.14$) reproduces without change the data at other energies except 56 MeV. Finally, Fig. 16 shows a more massive system, $^{40}Ca + ^{40}Ca$. The potential was adjusted to fit the data for 143.6 MeV and then used unchanged for the other energies.

Some special cases must be mentioned. First there are some systems at some energies analogous to the $\alpha + ^{40}Ca$ case just discussed which show relatively weak absorption and which are sensitive to the potential at radii smaller than the strong absorption radius. Data for one of these, $^{12}C + ^{12}C$ at energies from 70 to 126 MeV, was shown[34] to be fitted by using a deep, folded real potential, whereas good fits could not be obtained with a shallow potential. Another such case is $^{16}O + ^{28}Si$ at energies of ~ 50-70 MeV whose cross sections exhibit oscillations and relatively large values at back angles. This behaviour has been described[35] in terms of potential

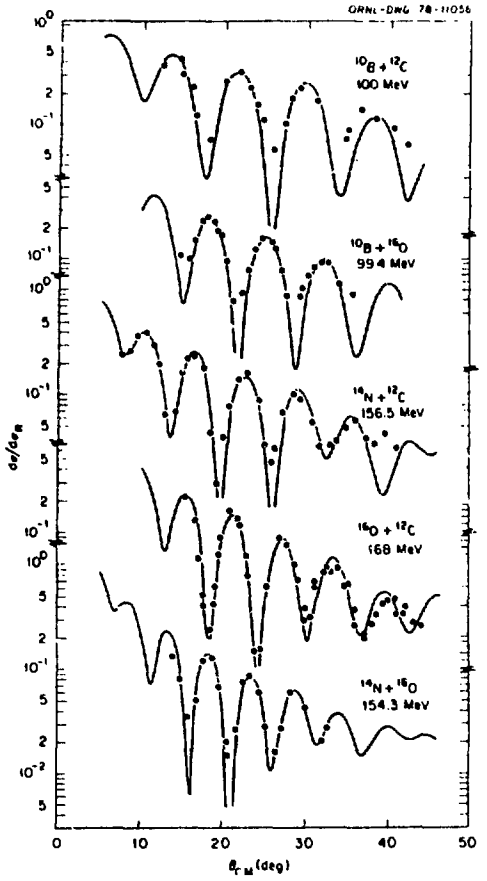

Fig. 13. Fits with folded real potentials and M3Y interaction (renormalized by N, Table 1).

scattering. The scattering from the folded potential can exhibit similar behaviour but not enough work has been done yet to know whether a good fit to these data can be achieved with it.

Finally, we must mention the scattering of ^{6}Li. Results for this projectile are not included in Table 1; however, analyses of ^{6}Li scattering from a variety of targets at energies from 23 to 156 MeV show[36] that the folding model with the M3Y interaction overestimates the ^{6}Li-nucleus potential by almost a factor of 2. (Most data are consistent with N ≈ 0.6.) This includes a case, ^{6}Li + ^{40}Ca at 30 MeV, which exhibits ALAS (see Fig. 17) and is sensitive to the potential at small radii, yet which is fitted well by simply renormalizing the folded potential by 0.6. The reason for this discrepancy is not yet understood, although it is likely to be related to the ease with which ^{6}Li may be broken up. The scattering of ^{7}Li has not yet received much study but does <u>not</u> appear to be anomalous in the same way.

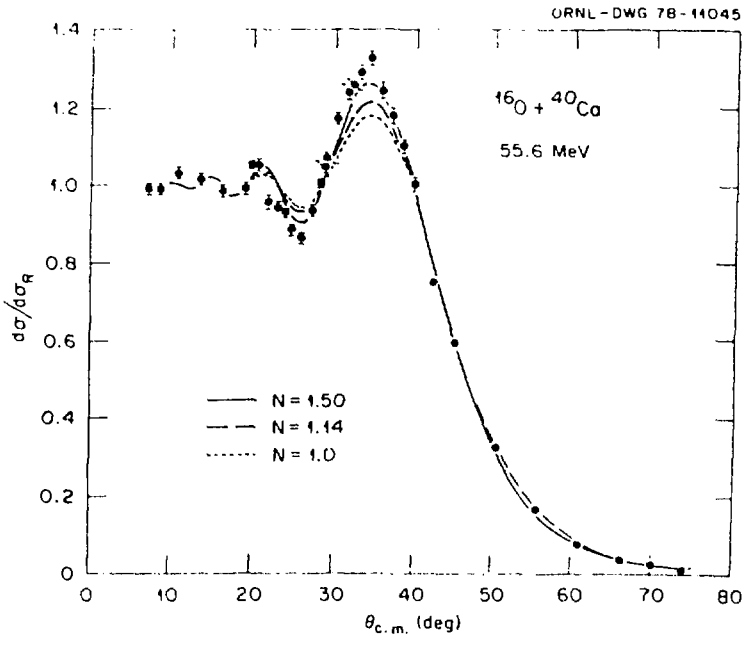

Fig. 14. Effect of varying the strength of the real, folded potential (obtained with the M3Y interaction).

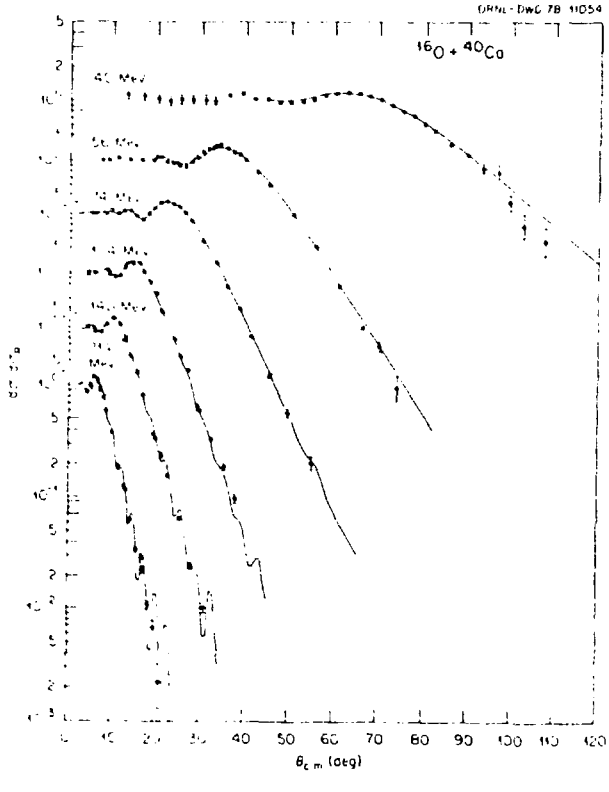

Fig. 15. Cross sections from folded real (M3Y) plus Woods-Saxon imaginary potential for $^{16}O + ^{40}Ca$. The potential was adjusted to fit the 74-MeV data (N = 1.14).

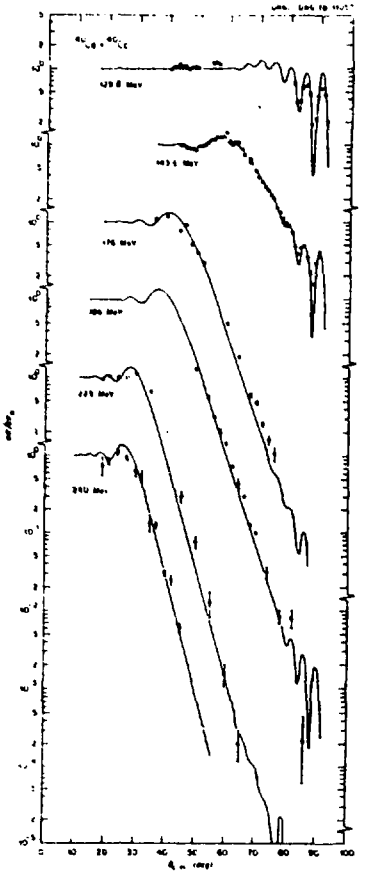

Fig. 16. Cross sections from folded real (M3Y) and Woods-Saxon imaginary potential for $^{40}Ca + {}^{40}Ca$. The potential was adjusted to fit the 143.6 MeV data.

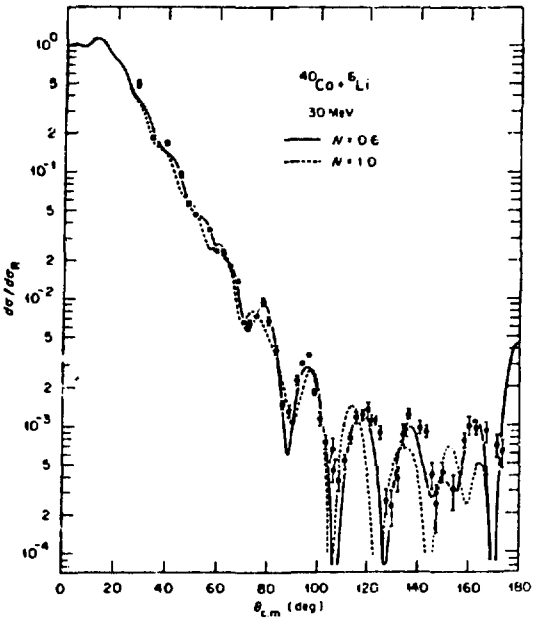

Fig. 17. Scattering from folded real (M3Y) plus Woods-Saxon imaginary potential for $^{6}Li + {}^{40}Ca$. Folded potential renormalized by N.

References

(Instead of attempting a complete bibliography, often I simply refer to papers where other references can be found.)

*Supported by a Research Fellowship of the Japan Society for the Promotion of Science.

**Research sponsored by the Division of Physical Research, U.S. Department of Energy, under contract W-7405-eng-26 with the Union Carbide Corporation.

1) See, for example, N. K. Glendenning in Proc. Int. School Phys., "Enrico Fermi", Course XL (Academic Press, New York, 1969); V. A. Madsen, in Nuclear Spectroscopy and Reactions, Part D (Academic Press, New York, 1975).

2) See, for example, M. H. Macfarlane, in Proc. Int. School Phys., "Enrico Fermi", Course XL (Academic Press, New York, 1969).

3) H. Feshbach, Ann. Phys. 19 (1967) 287.

4) J. P. Jeukenne, A. Lejeune and C. Mahaux, Phys. Rev. C16 (1977) 80.

5) F. A. Brieva and J. R. Rook, Nucl. Phys. A297 (1978) 206.

6) G. M. Lerner and E. F. Redish, Nucl. Phys. A193 (1972) 565; G. M. Lerner and J. B. Marion, Nucl. Phys. A193 (1972) 593.

7) W. G. Love and G. R. Satchler, Nucl. Phys. A159 (1970) 1.

8) D. Slanina and H. McManus, Nucl. Phys. 116 (1968) 271; L. W. Owen and G. R. Satchler, Phys. Rev. Lett. 25 (1970) 1720; G. R. Satchler, Zeit. f. Phys. 260 (1973) 209; E. C. Halbert and G. R. Satchler, Nucl. Phys. A233 (1974) 265.

9) G. E. Brown, Unified Theory of Nuclear Models and Forces (John Wiley & Sons, New York, 1967).

10) P. W. Coulter and G. R. Satchler, Nucl. Phys. A293 (1977) 269.

11) G. Baur, V. A. Madsen and F. Osterfeld, Phys. Rev. C17 (1978) 819.

12) See, for example, W. G. Love and L. J. Parish, Nucl. Phys. A157 (1970) 625; W. G. Love, Nucl. Phys. A192 (1972) 49.

13) F. A. Brieva and J. R. Rook, Nucl. Phys. A297 (1978) 206.

14) F. A. Brieva and B. Z. Georgier, to be published.

15) G. R. Satchler, Phys. Lett. 59B (1975) 121.

16) G. Bertsch et al., Nucl. Phys. A284 (1977) 399.

17) F. Petrovich et al., Phys. Rev. Lett. 22 (1969) 895.

18) W. G. Love and L. W. Owen, Nucl. Phys. A239 (1975) 74.

19) Y. Eisen and B. Day, Phys. Lett. 63B (1976) 253.

20) F. A. Brieva, H. V. Geramb and J. R. Rook, to be published.

21) D. E. Bainum et al., Phys. Rev. C16 (1977) 1377.

22) W. G. Love, Phys. Rev. C15 (1977) 1261.

23) W. G. Love and G. R. Satchler, Nucl. Phys. A101 (1967) 424; A172 (1971) 449.

24) F. Petrovich et al., Phys. Rev. C16 (1977) 839.

25) W. G. Love, submitted to Nucl. Phys.

26) Z. Majka et al., Phys. Rev. C18 (1978) 114.

27) See, for example, Gubler et al., Phys. Lett. 74B (1978) 202; see also Proc. Conf. on Radial Shape of Nuclei (Cracow, 1976).

28) B. Buck et al., Nucl. Phys. A275 (1977) 246.

29) F. Michel and R. Vanderpoorten, Phys. Rev. C16 (1977) 142.

30) D. M. Brink and N. Takigawa, Nucl. Phya. A279 (1977) 159.

31) W. G. Love, Phys. Rev. C17 (1978) 1876.

32) W. G. Love and G. R. Satchler, to be published.

33) H. Wojciechowski et al., Phys. Rev. C17 (1978) 2126.

34) R. M. Wieland et al., Phys. Rev. Lett. 37 (1976) 1458.

35) V. Shkolnik et al., Phys. Lett. 74B (1978) 195.

36) G. R. Satchler and W. G. Love, Phys. Lett. 76B (1978) 23.

37) P. J. Moffa, C. B. Dover and J. P. Vary, Phys. Rev. C16 (1977) 1857.

38) G. R. Satchler et al., Nucl. Phys. A298 (1978) 313.

39) W. G. Love, Phys. Lett. 72B (1978) 4.

Table 1. Heavy-ion scattering using a folded real potential based upon the M3Y interaction. The potential is multiplied by N and N is varied to optimise the fit to the data.

System	Energy (MeV)	N	System	Energy (MeV)	N
$^{40}Ca + ^{40}Ca$	130-240	1.32	$^{16}O + ^{28}Si$	142	0.91
$^{32}S + ^{48}Ca$	83	1.09	$^{16}O + ^{28}Si$	215	0.76
$^{32}S + ^{40}Ca$	100	1.26	$^{16}O + ^{28}Si$	81	1.00
$^{32}S + ^{32}S$	91	1.22	$^{16}O + ^{28}Si$	72	1.00
$^{32}S + ^{27}Al$	100	1.06	$^{16}O + ^{28}Si$	66	1.01
$^{16}O + ^{208}Pb$	313	1.05	$^{16}O + ^{28}Si$	60	1.01
$^{16}O + ^{208}Pb$	192	0.95	$^{16}O + ^{28}Si$	53	1.00
$^{16}O + ^{208}Pb$	130	1.16	$^{16}O + ^{28}Si$	38	1.01
$^{16}O + ^{88}Sr$	59	1.22	$^{16}O + ^{12}C$	168	1.11
$^{16}O + ^{88}Sr$	56	1.21	$^{15}N + ^{89}Y$	50	1.18
$^{16}O + ^{88}Sr$	52	1.19	$^{14}N + ^{16}O$	154	1.30
$^{16}O + ^{88}Sr$	48	1.36	$^{14}N + ^{12}C$	156	1.03
$^{16}O + ^{60}Ni$	142	1.00	$^{13}C + ^{207}Pb$	86	1.27
$^{16}O + ^{60}Ni$	61	1.04	$^{12}C + ^{208}Pb$	116	1.26
$^{16}O + ^{59}Co$	142	1.00	$^{12}C + ^{208}Pb$	96	1.25
$^{16}O + ^{59}Co$	56	1.00	$^{12}C + ^{142}Nd$	70	1.15
$^{16}O + ^{59}Co$	52	0.99	$^{12}C + ^{90}Zr$	98	0.98
$^{16}O + ^{59}Co$	49	1.10	$^{12}C + ^{40}Ca$	45	1.14
$^{16}O + ^{59}Co$	46	0.87	$^{12}C + ^{28}Si$	132, 186	0.97
$^{16}O + ^{59}Co$	40	0.98	$^{12}C + ^{28}Si$	40	1.02
$^{16}O + ^{48}Ca$	56	0.98	$^{12}C + ^{12}C$	70-126	1.01-1.13
$^{16}O + ^{40}Ca$	214	1.05	$^{11}B + ^{209}Bi$	75	1.45
$^{16}O + ^{40}Ca$	140	1.23	$^{11}B + ^{208}Pb$	72	1.26
$^{16}O + ^{40}Ca$	104	0.99	$^{10}B + ^{16}O$	99	1.04
$^{16}O + ^{40}Ca$	74	1.14			
$^{16}O + ^{40}Ca$	56	1.27	Average		1.09 ± 0.13